Tilt angle control of nanocolumns grown by glancing angle sputtering at variable argon pressures

J. M. García-Martín,[1,a] R. Alvarez,[2] P. Romero-Gómez,[2] A. Cebollada,[1] and A. Palmero[2]
[1]*IMM-Instituto de Microelectrónica de Madrid (CNM-CSIC), Isaac Newton 8, 28760 Tres Cantos, Madrid, Spain*
[2]*Instituto de Ciencia de Materiales de Sevilla, (CSIC-Universidad de Sevilla), Americo Vespucio 49, 41092 Seville, Spain*

(Received 20 July 2010; accepted 7 October 2010; published online 25 October 2010)

We show that the tilt angle of nanostructures obtained by glancing angle sputtering is finely tuned by selecting the adequate argon pressure. At low pressures, a ballistic deposition regime dominates, yielding high directional atoms that form tilted nanocolumns. High pressures lead to a diffusive regime which gives rise to vertical columnar growth. Monte Carlo simulations reproduce the experimental results indicating that the loss of directionality of the sputtered particles in the gas phase, together with the self-shadowing mechanism at the surface, are the main processes responsible for the development of the columns. © *2010 American Institute of Physics*. [doi:10.1063/1.3506502]

Glancing angle deposition (GLAD) is a versatile and powerful technique to obtain nanostructures in large areas and with a high variety of morphologies by exploiting atomic shadowing effects during physical vapor deposition.[1–6] Even though e-beam or resistively heated evaporation sources are commonly used for this purpose due to their high directionality, sputtering has also been used to obtain nanostructured systems by GLAD.[7–14] In this case, the sputtering gas pressure, P_g, is obviously a crucial parameter in the formation of the columnar structures, trying to be minimized in order to reduce the number of collisions of the sputtered atoms in the gas phase and therefore to increase the directionality of the sputtered material toward the substrate.

P_g determines the mean free path, λ, of the vapor flux that leaves the target in their way to the substrate. Since this magnitude roughly ranges from 1 cm to 1 m between 10^{-2} and 10^{-4} mbar, it is obvious that in a standard size deposition system, varying the Ar pressure between these ranges will allow tuning the mean free path of the sputtered atoms between the diffusive (multiple collision) and ballistic (collisionless) regimes, therefore modifying the degree of directionality and as a consequence the effective shadowing effects characteristic of the GLAD technique. For this, the use of a heavy atom with respect to Ar, for example Au, is convenient since it allows extending P_g to larger values with respect to lighter species, which would lose their directionality at lower pressures.

In this paper, we have studied the influence that Ar gas pressure has on the columnar growth of gold nanostructures obtained by GLAD magnetron sputtering, and we have compared the obtained morphologies with theoretical simulations. The Au vapor flux is produced by magnetron sputtering of a 3.8 cm diameter gold target using argon as sputter gas. The base pressure of the chamber is in the mid 10^{-9} mbar range and the 2 cm^2 substrate of ultrasonically cleaned Si(100) is placed at $L=19$ cm from the target, and tilted 85° with respect to its normal. P_g was varied from 1.5×10^{-3} to 4×10^{-2} mbar, with the power and the deposition time being kept constant at 100 W and 1800 s, respectively. We have checked that the film temperature during the sputtering process was always below 350 K. Estimating the cross-section for an elastic scattering of a Au atom on an Ar atom by the geometrical cross-section ($\sigma_g=3.25\times10^{-19}$ m^2), the ratio L/λ can be calculated as $L/\lambda\sim800\times p_g$ (with p_g the Ar pressure in millibar and using a gas temperature of 600 K), which determines the number of collisions experienced by the Au atom until it is deposited.[15] In this way, the quantity $\Xi=L/\nu\lambda$, with ν being the average number of collisions required to thermalize the sputtered atoms, estimates the thermalization degree of the deposition flux. Since for Au atoms with initial kinetic energy of 5 eV in Ar the value of ν is $\nu=12$ (see Ref. 15 for more details), the value of $L/\nu\lambda$ in our conditions ranges from $\Xi(p_g=1.5\times10^{-3}$ mbar$)\sim0.1$ to $\Xi(p_g=4\times10^{-2}$ mbar$)\sim2.7$. In this way, when $\Xi\geq1$ (i.e., for deposition pressures above ~0.015 mbar), most of the Au atoms in the gaseous phase are thermalized with the background gas, and therefore they reach the substrate with an isotropic velocity distribution function.[15]

Figure 1 shows cross-sectional scanning electron micrograph images of the deposited samples illustrating the effect of varying the Ar pressure during the deposition. Figure 1(a) corresponds to a sample grown with 1.5×10^{-3} mbar of Ar. With this pressure and the geometrical parameters previously mentioned, the sputtered Au atoms experience in average about one collision in their way to the substrate, so the deposition takes place in the so-called *low pressure long throw* sputtering regime that increases the collimation with respect to conventional sputtering.[16,17] Due to the self-shadowing effect and the low adatom diffusion compared to the Au atoms arrival time for the used deposition conditions, nanostructures that are elongated along the flux direction are formed. The column tilt angle, β, is always smaller than the deposition angle (85°), with $\beta=62°$ in this case. In Figs. 1(b)–1(d), we find similar columnar structures whose tilt angle decreases with the value of the deposition pressure: $\beta=38°$ for 1×10^{-2} mbar ($\Xi\sim0.67$), $\beta=16°$ for 2.5×10^{-2} mbar

[a]Electronic mail: jmiguel@imm.cnm.csic.es.

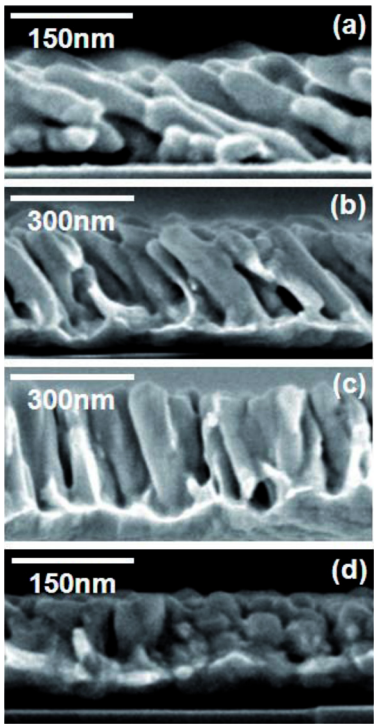

FIG. 1. (Color online) Field enhanced scanning electron micrograph images for samples prepared by GLAD sputtering at 85° off-normal with different Ar pressure: (a) 1.5×10^{-3} mbar, (b) 1×10^{-2} mbar, (c) 2.5×10^{-2} mbar, and (d) 4×10^{-2} mbar.

($\Xi\sim1.69$), and finally the columns grow perpendicular to the substrate for 4×10^{-2} mbar ($\Xi\sim2.7$).

The relation between the tilt angle and the incidence angle has been theoretically studied for many different materials and under several deposition conditions. Nieuwenhuizen and Haanstra[18] found a phenomenological relation between the column tilt angle, β, and the deposition angle, α, as $\tan(\beta)=0.5\tan(\alpha)$, that overestimates the former for increasingly oblique deposition (for $\alpha=85°$ it gives $\beta=80°$). On the other hand, Tait *et al.*[19] assumed ballistic deposition and shadow effects leading to the relation $2\times\sin(\alpha-\beta)=1-\cos(\alpha)$, that for $\alpha=85°$ gives $\beta=58°$, i.e., closer to our experimental value. Some other models have introduced additional parameters depending on the deposition rate or the diffusivity.[20,21] However, none of them are suitable for reproducing the experimental evolution illustrated in Fig. 1: this has motivated us to develop a model that permits the calculation of β as a function of the deposition pressure. The better agreement with the model of Tait *et al.* for the lowest pressure case gives clues about the importance of the surface shadowing. On the other hand, the abovementioned model does not consider any modification of the incident angle distribution function of the deposition particles due to scattering processes in the gaseous phase, thus no deposition pressure dependence is taken into account. In order to understand the influence of P_g on the development of the thin film nanostructure, we have solved a Monte Carlo ballistic model using diverse calculated incident angle distribution functions in various conditions.

We consider the deposition of Au atoms on a two-dimensional substrate that defines the x-y plane, whereas the z axis is defined by the direction perpendicular to the substrate. The three-dimensional space is divided into a $N_L\times N_L\times N_H$ grid and each atom moves toward the substrate from an initial random position following the direction defined by the spherical angles θ and φ, where $\theta\in[0,\pi/2)$ is the polar angle ($\theta=0$ is the direction normal to the substrate) and $\varphi\in[0,2\pi)$ is the azimuthal angle. The movement of the particle continues, assuming periodic boundary conditions, until it hits the surface, where it sticks. The angles θ and φ are randomly calculated by defining an incident angle distribution function per unit time and unit surface, $I(\Omega)$, with $d\Omega=\sin\theta d\theta d\varphi$ being the differential solid angle.[22,23] We have not introduced surface diffusion nor desorption mechanisms, due to the low temperature of the film during growth.

In order to estimate the magnitude $I(\Omega)$ as a function of P_g we have employed the SIMTRA code with parameters that deal with the system geometry (tilt angle of the substrate, target size, target-sample distance, dimensions of the reactor) and the deposition conditions (P_g, gas temperature, nature of the sputtered species).[24] The interaction potential between the Au and the Ar atom was considered a Molière type, and three possible values of the spatially averaged gas temperature were considered: 500, 600, and 700 K. In general, gas temperature is not constant along the plasma discharge; the heating of gas particles caused by the collisions with the sputtered particles introduce important gas temperature gradients, with the cathode temperature depending in a great deal on the cooling efficiency. In this way, numerical and experimental estimations have obtained cathode temperatures around and above 700 K, whereas the film temperature remains below 400 K.[15,25] Furthermore, elastic collisions between sputtered and gas atoms heat up the gas specially at a distance of about λ, where temperatures far above the cathode temperature can be found.[26,27] Once the function $I(\Omega)$ is calculated, the model is solved for values of N_L up to 2000 (in order to avoid finite size effects in the solutions) and $N_H=500$.

Results of the model for a gas temperature of 600 K and for the same deposition pressures as in Fig. 1 appear in Fig. 2. There, we show a columnar structure with tilt angle depending on P_g: for $P_g=1.5\times10^{-3}$ mbar [Fig. 2(a)] we find tilted columns which become wider for increasing values of the film thickness. For $P_g=1\times10^{-2}$ mbar [Fig. 2(b)], the column tilt angle decreases, which becomes more evident for $P_g=2.5\times10^{-2}$ mbar [Fig. 2(c)]. Finally for $P_g=4\times10^{-2}$ mbar [Fig. 2(d)], columns grow perpendicular to the substrate, which is coherent with an isotropic incident angle distribution function of the deposition particles. Tilt angle as a function of Ξ appears in Fig. 3 for different values of the spatially averaged gas temperature in the discharge; model results match quite well with the experimental values of β. Furthermore, resulting curves overlap in the whole studied range no matter the gas temperature, indicating that the parameter defining the tilt angle is Ξ. In order to study if this result can be generalized, in Fig. 3 we have also included calculated results for the sputtering of Ag and Cu in Ar, considering two different gas temperatures (500 and 700 K) and different values of L. In these cases $\nu=6.6$ for Ag and $\nu=3.6$ for Cu, which are coherent with the lower masses of Ag and Cu in comparison with that of Au (see Ref. 15 for more details). Figure 3 shows that all the calculated data overlap, indicating that our results are general irrespective of the gas temperature, the distance cathode-film or the composition of the film.

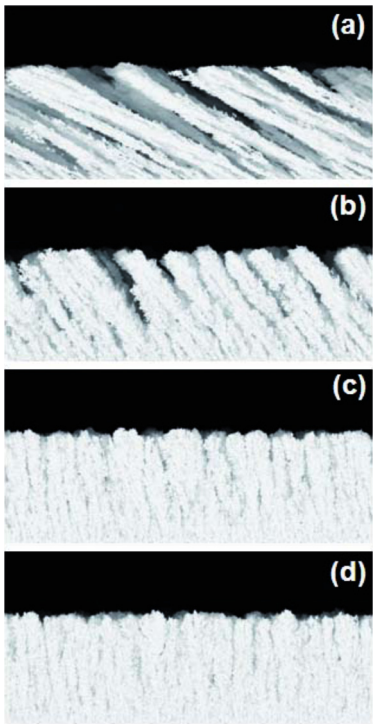

FIG. 2. (Color online) Solutions of the model using the different incident angle distribution function for various deposition pressures and a gas temperature of 600 K: (a) 1.5×10^{-3} mbar, (b) 1×10^{-2} mbar, (c) 2.5×10^{-2} mbar, and (d) 4×10^{-2} mbar.

In summary, we have shown how the Ar pressure in GLAD sputtered Au structures strongly influences the degree of directionality of the impinging Au atoms, and as a consequence, the morphology and inclination of the resulting nanocolumns. The inclination of these columns with respect to the substrate normal changes from zero for high Ar pressures, where the Au atoms are thermalized in the gas phase, to 62° for low Ar pressures, where the Au trajectories are mainly ballistic. The developed theoretical model supports these experimental findings and explains that the main processes responsible for the formation of the nanostructure of these films are the self-shadowing mechanisms at the surface and the collisional processes of the sputtered particles in the gas phase. This is a universal process, theoretically observed also for other sputtered materials and gas temperatures.

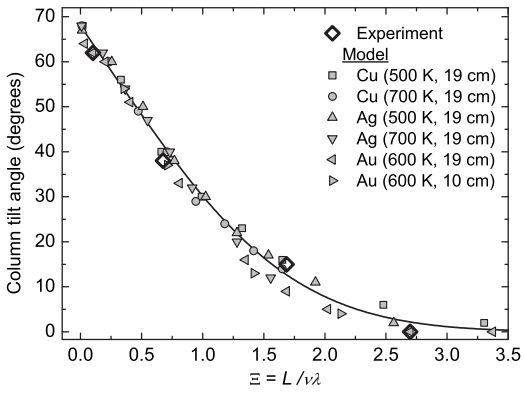

FIG. 3. Result of the calculation of the tilt angle as a function of the parameter $\Xi = L/\nu\lambda$ for Au, Ag, and Cu for different gas temperatures and values of L, along with the experimental data for Au. A numerical fit to the calculated data has also been included as a visual guide (solid line).

Financial support from the Spanish MICINN (Grant Nos. CSD 2008-00023, MAT 2008-06765-C02-01/NAN, MAT 2007-65764, and PIE 200960I132), Comunidad de Madrid (Grant No. S2009/MAT-1726), Junta de Andalucía (Grant Nos. TEP2275 and P07-FQM-03298) and European Commission (Grant No. NMP3-SL-2008-214107) is acknowledged. R. Álvarez acknowledges the JAE Program of CSIC.

[1]K. Robbie and M. J. Brett, J. Vac. Sci. Technol. A **15**, 1460 (1997).
[2]R. Messier, V. C. Venugopal, and P. D. Sunal, J. Vac. Sci. Technol. A **18**, 1538 (2000).
[3]M. M. Hawkeye and M. J. Brett, J. Vac. Sci. Technol. A **25**, 1317 (2007).
[4]K. Robbie, J. C. Sit, and M. J. Brett, J. Vac. Sci. Technol. B **16**, 1115 (1998).
[5]B. Dick, M. J. Brett, T. J. Smy, M. R. Freeman, M. Malac, and R. F. Egerton, J. Vac. Sci. Technol. A **18**, 1838 (2000).
[6]B. Dick, M. J. Brett, and T. J. Smy, J. Vac. Sci. Technol. B **21**, 23 (2003).
[7]D. Le Bellac, G. A. Niklasson, and C. G. Granqvist, Europhys. Lett. **32**, 155 (1995).
[8]B. Dick, M. J. Brett, T. Smy, M. Belov, and M. R. Freeman, J. Vac. Sci. Technol. B **19**, 1813 (2001).
[9]T. Karabacak, J. P. Singh, Y.-P. Zhao, G.-C. Wang, and T.-M. Lu, Phys. Rev. B **68**, 125408 (2003).
[10]F. Tang, T. Karabacak, L. Li, M. Pelliccione, G.-C. Wang, and T.-M. Lu, J. Vac. Sci. Technol. A **25**, 160 (2007).
[11]C. M. Zhou and D. Gall, J. Appl. Phys. **103**, 014307 (2008).
[12]C. M. Zhou, H. F. Li, and D. Gall, Thin Solid Films **517**, 1214 (2008).
[13]C. Patzig, T. Karabacak, B. Fuhrmann, and B. Rauschenbach, J. Appl. Phys. **104**, 094318 (2008).
[14]C. Patzig, A. Miessler, T. Karabacak, and B. Rauschenbach, Phys. Status Solidi B **247**, 1310 (2010).
[15]A. Palmero, H. Rudolph, and F. H. P. M. Habraken, J. Appl. Phys. **101**, 083307 (2007).
[16]D. Liu, S. K. Dew, M. J. Brett, T. Janacek, T. Smy, and W. Tsai, Thin Solid Films **236**, 267 (1993).
[17]J. N. Broughton, M. J. Brett, S. K. Dew, and G. Este, IEEE Trans. Semicond. Manuf. **9**, 122 (1996).
[18]J. M. Nieuwenhuizen and H. B. Haanstra, Philips Tech. Rev. **27**, 87 (1966).
[19]R. N. Tait, T. Smy, and M. J. Brett, Thin Solid Films **226**, 196 (1993).
[20]S. Lichter and J. Chen, Phys. Rev. Lett. **56**, 1396 (1986).
[21]I. Hodgkinson, Q. H. Wu, and J. Hazel, Appl. Opt. **37**, 2653 (1998).
[22]M. Pelliccione and Toh-Ming Lu, *Evolution of Thin Film Morphology* (Springer, Berlin, 2008).
[23]R. Álvarez, A. Palmero, L. O. Prieto-López, F. Yubero, J. Cotrino, W. de la Cruz, H. Rudolph, F. H. P. M. Habraken, and A. R. Gonzalez-Elipe, J. Appl. Phys. **107**, 054311 (2010).
[24]K. Van Aeken, SIMTRA, available at http://www.draft.ugent.be/.
[25]A. Bogaerts and R. Gijbels, J. Anal. At. Spectrom. **19**, 1206 (2004).
[26]A. Palmero, H. Rudolph, and F. H. P. M. Habraken, Appl. Phys. Lett. **87**, 071501 (2005).
[27]A. Palmero, H. Rudolph, and F. H. P. M. Habraken, Thin Solid Films **515**, 631 (2006).